Chapter 3
Nanotribology and Wettability of Molecularly Thin Film

Yufei Mo and Liping Wang

Abstract The micro/nano-electromechanical systems (MEMS/NEMS) have received rapid development in the past decades due to their superior performance and low unit cost. However, large surface area-to-volume ratio causes serious adhesive and frictional problems for MEMS operations. Nanotribology is a study of the interaction between contact surfaces at nanoscale, from chemistry and physics to material science and mechanical engineering, and is of extreme technological importance to the application and development of MEMS. This chapter will attempt to cover the range from preparation of organic thin films to instruments and measurement protocols. We will describe this process in steps. The preparation of thin film materials (i.e., ionic liquids, multiply-alkylated cyclopentane or self-assembled molecules) and film deposition are presented. Also, the methods of film evaporation are considered. We examined the relationship of adhesion and lateral force data to their fundamental aspects at molecular level. The main objective will be to provide more thorough examination to the interested reader, and to provide a source to further raise the critical issues concerning the relationship between surface properties and MEMS application. Fluorinated molecules with coplanar structure were successfully self-assembled onto silicon surface. The fluorinated monolayers possessed excellent adhesion-resistance, friction-reduction and anti-wear durability, which were attributed to low interfacial energy of end group and dual layer structure of the films. The spatial distribution of the multi-component film was evaluated by adhesion statistic measurement. Multialkylated cyclopentanes (MACs) are potential lubricants for space and MEMS application due to their extreme low volatility. A series of MACs were synthesized by Dean-Stark trap, autoclave, and phase transfer catalysis methods. Nanoscale dual-layer films consisting of both MACs and self-assembled monolayers (SAMs) were prepared and their morphology, wettability and tribological properties were investigated. Molecularly thin ILs films with different molecular

Y. Mo · L. Wang (✉)
State Key Laboratory of Solid Lubrication, Lanzhou Institute of Chemical Physics,
Chinese Academy of Sciences, Lanzhou 730000, P. R. China
e-mail: lpwang@licp.cas.cn

S. K. Sinha et al. (eds.), *Nano-tribology and Materials in MEMS*,
DOI: 10.1007/978-3-642-36935-3_3,

structures which showed excellent tribological performance were designed, synthesized and prepared successfully on silicon surface by dip-coating method. The influences of anion, cation and post-treatment on wettability and tribological properties of ILs films were investigated systematically. To enhance the wettability and to improve the nanotribology of nano films, surface texture technique is reviewed. Regular and biomimetic surface textures were fabricated by local anodic oxidation (LAO). Dimension of the pillars were precisely controlled by operation parameters such as pulse bias voltage, pulse width and humidity. The H-passivated Si showed higher growth rate and thicker saturated oxide film than common p- or n-type Si under the same oxidation condition. The H-passivated Si employed in LAO process can improve lateral resolution of patterns. The adhesive and friction force of LAO pattern were measured by AFM colloidal probe. The friction forces are closely related to the surface coverage of the nanotexture. The results indicate that nanotextures significantly reduced the friction force, while H-passivated Si showed large friction force, this is because of the less adhesive energy dissipated during sliding on textured surface. The surface nanotextures of biological origins were fully duplicated on surface based on duplication method. The morphology and the size of the surface textures of the replicas are almost in accordance with their biological sources. The wettability of the surfaces was improved with hydrophobicity after duplicating with textures. And the biomimetic textures have shown to improve nanotribological performance.

Contents

Introduction

The microelectromechanical systems (MEMS) have received rapid development in the past decades due to their superior performance and low unit cost. However, large surface area-to-volume ratio causes serious adhesion and frictional problems for MEMS operations. In MEMS devices, various forces associated with the device scale down with the size. When the length of the machine decreases from 1 mm to 1 μm, the area decrease by a factor of million and volume decreases by a factor of a billion. At this scale, mechanical loading is often not the overwhelming force as in macroscale, and surface forces such as van der Waals, electronic and capillary force that are proportional to area, become a thousand times larger than the forces proportional to volume. In addition to the consequence of a large area-to-volume ratio since MEMS devices are designed for small tolerance, physical contact becomes more likely, which makes them particularly vulnerable to adhesion between adjacent components. Slight particulate or chemical contamination present at the interface can lead to failure. Since the start up forces and torques involved in operation available to overcome retarding forces are small in MEMS, the increase in resistive forces such as adhesion force and lateral friction force become a serious tribological concern that limits the durability and reliability in MEMS. A large friction force is required to initiate relative motion between two surfaces, that is large static friction, which has been thoroughly studied in the field of data magnetic storage. The adhesion is generally measured by the amount of force necessary to separate two surfaces in contact. Adhesion, friction, wear can affect MEMS performance and even lead to failure.

Space lubrication and nanotechnology are driven by the trends such as device miniaturization, better integrated functional components and energy saving properties. MEMS as miniaturized devices are operated under very narrow space and small normal load. They cannot be lubricated with lubrication oils, but usually employ thin films whose thickness is well below a few nanometers. The adhesive force comes largely from meniscus force and viscous force, rather than the applied loads. The perfluoropolyether (PFPE) thin films are the most widely used lubricants in data storage devices, but PFPEs usually experience metal catalytic degradation and are normally expensive. The potential of self-assembled monolayers (SAMs), multiplyalkylated cyclopentanes (MACs) and ionic liquids (ILs) as thin lubricant films were exploited by a number of researchers aiming to replace PFPEs. The molecular structure, length of alkyl chains, functional groups, surface microstructure and substrate modification are key factors which affect the wettability and the nanotribological behavior of these thin films.

Tribological Behavior of Perfluorinated Carboxylic Acid and Hydrogenated Carboxylic Acid SAMs

Molecular thin films of several monolayers or less supported by surfaces exhibit considerable departure from bulk behavior, which is mainly due to molecular alignment or ordering. SAMs have been widely investigated during the past decade because of their potential applications in the field of surface modification, boundary lubricant, sensor, photoelectronics, and functional bio-membrane modeling etc. On the basis of the synthetic approaches and the surface chemical reactions, the chemical structures of SAMs can be altered easily both at the individual molecular and at the material levels. The nanotribological properties of SAMs, which are potential lubricants for controlling adhesion and friction, are closely related to their intrinsic chemical composition and structure. For example the friction behaviors of SAMs are termina group and chain length dependent. SAMs with long chains are generally densely packed, while the shorter chain ones are not. With the same terminal group, loosely packed SAMs generally posses higher friction force due to the large energy dissipation during the relative movement, and adhesive force as well due to the liquid-like disordered structure. On the other hand, altering the terminal group, from apolar to polar, could result in the increase of adhesion and friction. This is because SAMs with more relatively strong interaction during the relative movement, and therefore higher adhesion and more energy loss are expected, which leads to a higher friction force. Mix-deposition of molecules with different terminal group or alkyl chain lengths to form mixed SAMs is also extensively studied, which allows an understanding of the relationship between structure and performance of SAMs in wide and depth.

As an example of tribological behavior of perfluorinated and hydrogenated carboxylic acid (FC and HC) SAMs on aluminum surface by chemical vapor deposition were studied [1]. Figure 3.1 shows the mechanism of adsorption of SAMs. The samples were placed in a 100 ml sealed vessel with a glass container filled with 0.2 ml FC or HC precursor. There was no direct contact between the samples and precursor. The vessel was placed in an oven and then nitrogen gas was filled in the oven. The samples were annealed in nitrogen at 200 °C for 3 h, and then cooled in a desiccator. The precursor vaporized and reacted with substrate surface on each sample, resulting in the formation of SAM. Then, the samples were rinsed with chloroform, acetone, ethanol, and deionised water successively to remove other physisorbed ions and molecules. The deposition of SAMs relied on the chemisorption of reactive head groups presented in the adsorbate molecules on the substrate surface in order to anchor them.

X-ray photoelectron spectroscopy (XPS) was used to evaluate the relative atomic composition on the surface of SAMs. The procedure involved the measurement of the Al2p, F1 s and C1 s core level spectra for surfaces of these films. The data of Al2p features from bare surface are shown in Fig. 3.2a and are associated with Al_2O_3 or AlO(OH) (74.7 eV) and Al (72.7 eV). This result indicates that the outmost layer of Al is converted to aluminum oxide under ambient

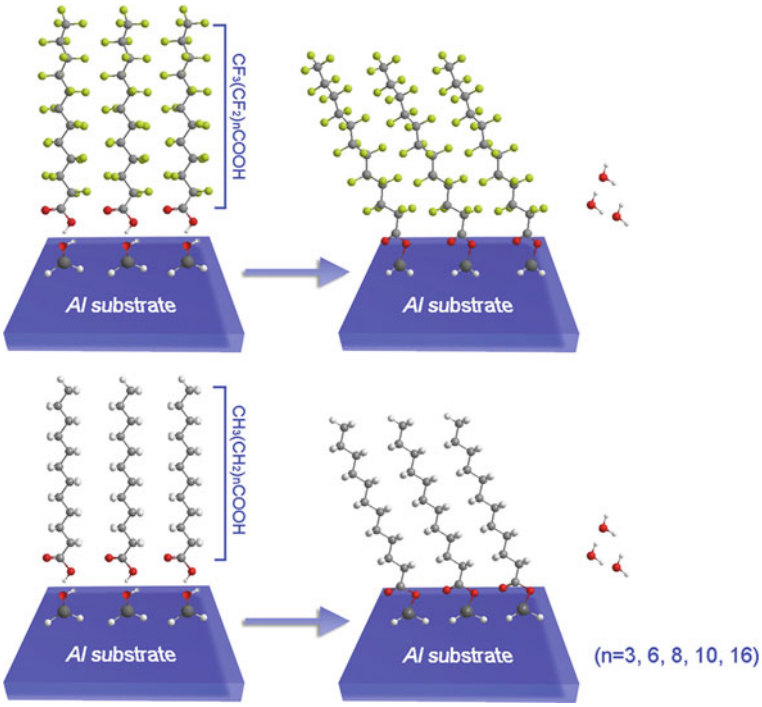

Fig. 3.1 Schematic structure and forming process of perfluorinated carboxylic acid and hydrogenated carboxylic acid molecules chemically adsorbed onto aluminum substrate. Perfluorinated carboxylic acid and hydrogenated carboxylic acid SAMs are of similar chain length and head group monolayers with different backbone groups. Reproduced with permission from Ref. [1]. Copyright (2009) Surface and Interface analysis

condition. A single F1s feature resulting from FC18 adsorption on aluminum oxide is shown in Fig. 3.2b. The F1s feature at 688.7 eV is assigned to $–CF_2–$and $–CF_3$ groups, which indicates the fluorine element on the substrate surface. Figure 3.2c displays the C1s spectra obtained from one set of FC SAMs with various chain lengths (C5–C18) on aluminum oxide surface. The C1s features are assigned to $–CF_3$ group ($\sim$293.5 eV), $–CF_2–$group (C5: 292.1–C18: 291.5 eV) [2, 3], carboxylate group (COO−, 289.2 eV), [4] and a feature (284.8 eV) associated with adventitious carbon possibly from airborne hydrocarbon contamination. It is suggested that the samples were strongly bonded with airborne organics (fatty acid, etc.), which were adsorbed at film defects and imperfections and were not easily removed by vacuum pumping. It is also observed that the intensity of adventitious carbon decreased rapidly with increase of fluorocarbon chain length while that of COO^- and $–CF_3$ remained constant. This is because the long chain FC– SAMs were densely packed and with fewer defects, which prevented airborne organics from adsorbing onto the film. Figure 3.2d shows a similar tendency of increase in C concentration associated with the increase of chain length in

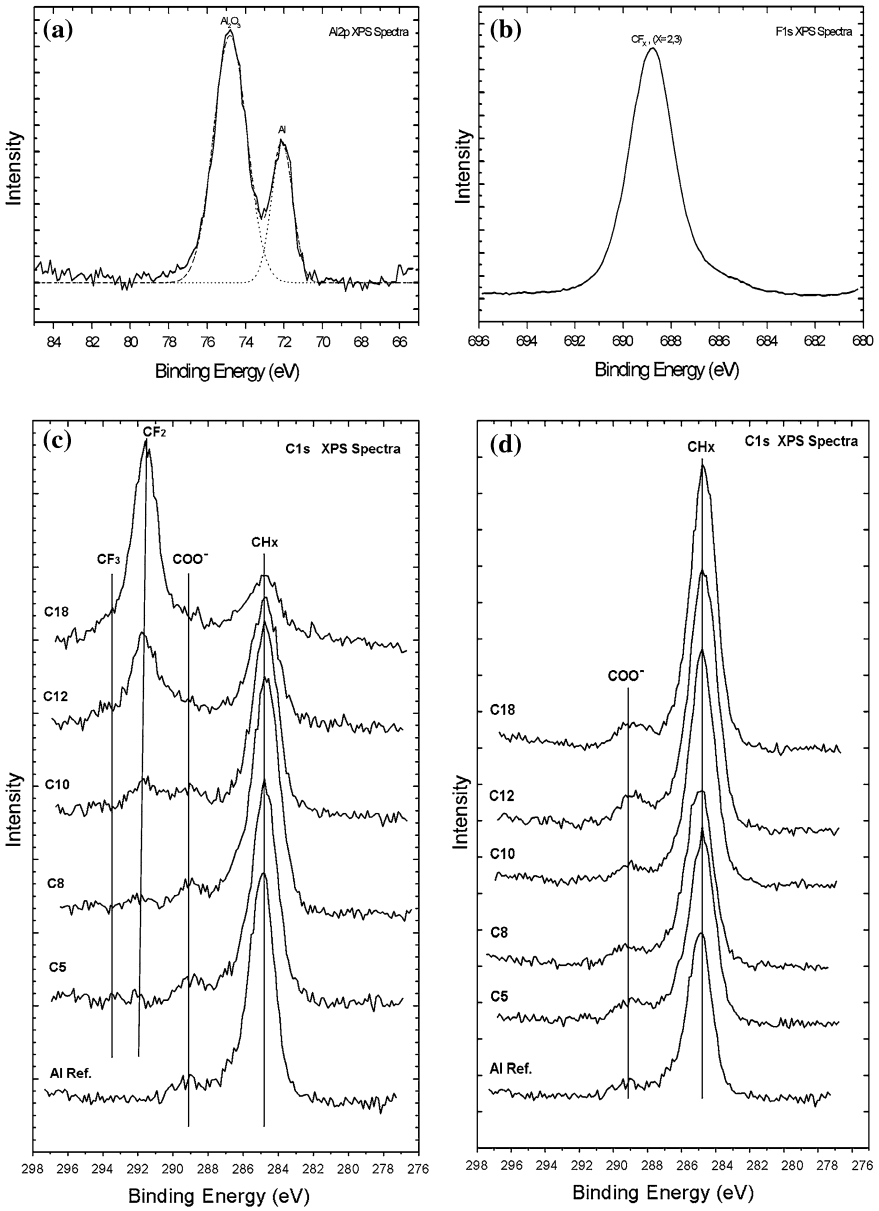

Fig. 3.2 XPS spectra of Al 2p **a** F 1s, **b** C1s, **c** region of the FC5-FC18 SAMs, **d** C 1s region of the HC5-HC18 SAMs. Reproduced with permission from Ref. [1]. Copyright (2009) Surface and Interface analysis

HC-SAMs. In addition, two features arose from C1s, as shown in this figure, the left feature assigned to carboxylate group (COO, 289.2 eV) and the right feature can be attributed to CHx (284.8 eV).

Nanotribological Properties of Monolayers Under Ambient Condition: Effect of Temperature and Humidity

The adhesive force between AFM tip and SAM surfaces under various relative humidity are shown in Fig. 3.3a and b. The bare aluminum surface showed higher adhesive force than SAMs deposited on it. Between FC and HC SAMs, the FC-SAMs showed lower adhesion force than HC-SAMs with same chain length, which indicates that adhesive force is consistent with the difference in surface energy (15 mJ/m^2 for CF_3-terminated compared to 19 mJ/m^2 for CH3-terminated SAMs [5]). The relationship between adhesive forces for bare Al and FC-SAMs with various chain lengths is shown in Fig. 3.3a. It shows that adhesive force

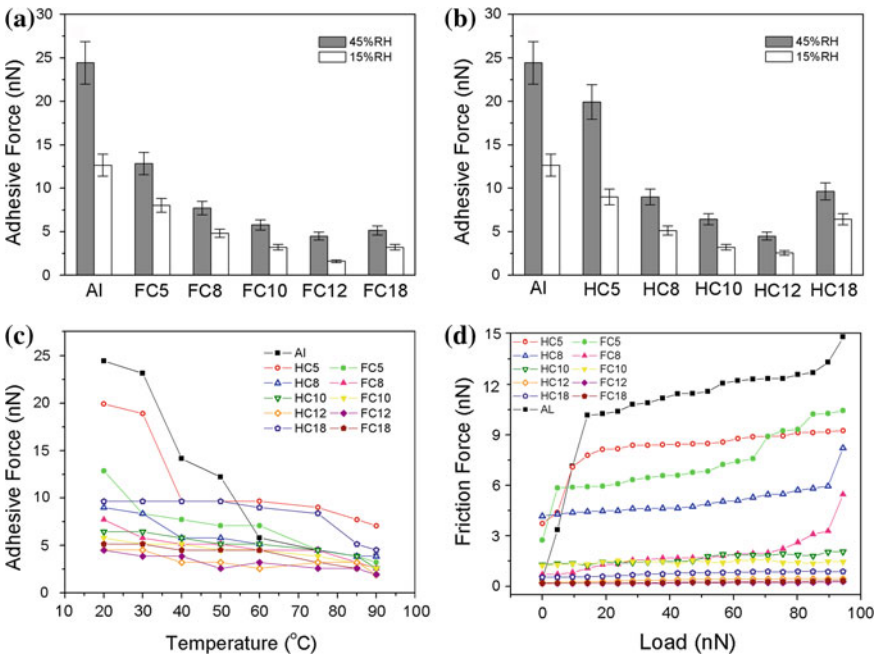

Fig. 3.3 Relative humidity dependence of adhesion for Al substrate and various SAMs. **a** FC-SAMs. **b** HC-SAMs. **c** Dependence on temperature of adhesion for the Al substrate, FC-SAMs (*solid symbols*) and HC-SAMs (*empty symbols*). **d** Plots of friction force versus load for various SAMs on Al substrate, FC-SAMs and HC-SAMs. Reproduced with permission from Ref. [1]. Copyright (2009) Surface and Interface analysis

increased with relative humidity (RH), which is due to water menisci contribution. It is also observed that the adhesive force of FC-SAMs with chain lengths up to ten carbons increased indistinctively and then tended to a stable value. This tendency of the adhesive force agrees well with the change in contact angles which correlates with surface energy [1]. FC12 and FC18 SAMs showed lowest adhesive forces and highest contact angles, which implies that 12-carbon and 18-carbon chains are prone to form more stiff film. In the case of short chain SAMs (n-carbon <10), they formed relatively soft monolayers and tended to disorder under the pressure applied by AFM tip. The pressure induced terminal defects may be sufficient for complete disorder, an effect that will be magnified by the reduced packing density of the short molecules. For SAMs with chain lengths up to ten carbons, low adhesive force may be attributed to high stiffness, which gives rise to a smaller contact area for the same applied load. Figure 3.3c shows the influence of temperature on adhesion. The adhesive force decreased with increase of temperature and then tended to a stable value. The drop in adhesive force is a result of desorption of water molecules and the corresponding decrease of water menisci contribution. The aluminum substrate and short chain SAMs showed more temperature dependence compared with long chain SAMs. The FC and HC SAMs with long chains exhibit temperature independence over the temperature range studied, which is due to the fact that highly hydrophobic nature of these monolayers results in less formation of water menisci. It indicates that long backbone chains and neighboring fluorine atoms provide stronger inter-chain interaction compared to that provided by short backbone chain and hydrogen atoms. SAMs with perfluorinated long chains were densely packed and highly ordered with solid-state-like properties at high temperature due to strong inter-chain van der Waals force.

Figure 3.3d shows the relationship between friction force and external load for bare Al, as well as for FC and HC SAMs with various chain lengths, at RH of 15 % and temperature of 20 $^{\circ}$C. The bare aluminum surface without organic film generates the highest friction. This may be attributed to the highest surface energy on the Al_2O_3-covered surface. The highest surface energy can be indicated by the lowest contact angle. It is a general tendency that the friction force decreases as chain length increases and FC-SAMs showed lower friction force than HC-SAMs of corresponding chain length. It is also observed that the friction properties of SAMs do not depend only on the chemical nature of terminal groups. Otherwise, all chain lengths should yield similar friction values. For the formation of SAMs, both surface energy and Inter-chain interactions play important roles and determine quality and character of the SAMs [6]. The decrease of friction is mainly due to SAMs with longer chain, as they generally possess relatively stronger inter-chain interaction, which give rise to a smaller contact area for the same applied load during the sliding. Tribological characterization studies of the SAMs can be summarized as shown in Table 3.1 [1].

Table 3.1 Summary of tribological properties for the FC arid HC SAMs on Al surface

	SAMs property	Adhesive force	Nanofriction	Microfriction
Backbone style	Fluorocarbon backbone	Low	Low	High
	Hydrocarbon backbone	High	High	Low
Chain length	Short ($Q < 10$)	High	High	–
	Middle ($C_n = 10–12$)	Low	Low	–
	Long ($C_n > 12$)	Low	Low	–
Terminal group	Methyl	High	High	Low
	Perfluorinated methyl	Low	Low	High

Structural Forces due to Surface Structure: Preparation and Tribological Properties of Perfluorinated Carboxylic Acid Dual-Layer SAMs

SAMs have good anti-rupture properties due to their strong bonding to the substrate surface, and they are expected not to freely migrate on the surface. However, some molecules from SAMs may transfer to the surface of counterpart when external force was applied on the contacting surface [7]. Because of monolayer structure and flexibility, SAMs exhibit poor anti-wear durability [8–10]. To utilize SAMs as lubricants to protect MEMS, it is necessary to consider the molecule layer structure as well as the strongly bonded characteristics of lubricant [11]. Generally, there are two approaches to obtain these more complex structures on surface: one is to synthesize target precursors with functional groups and then assemble them onto surfaces by a one-step method, [12–17] but there are difficulties in purification during the synthesis of more complex molecules. Another is stepwise formation of the film with desired structures based on surface chemical reaction.

Several reports [13–15] have demonstrated that incorporation of amides into hydrocarbon backbones of precursor could improve the stability of SAMs. The reason was that the amide underlayers were capable of being cross-linked by hydrogen bonding. Work has also recently been done on building amide-containing dual layer SAMs on silicon surfaces and found to be very excellent wear-resistant films [16, 17]. Bai et al. [18] designed a perfluorinated dual layer structure which can help to improve the film quality, reduce the friction and significantly enhance their durability, as shown in Fig. 3.4.

A self-assembled dual-layer film was prepared on single-crystal silicon surface by chemisorption of perfluorododecanoic acid (PFDA) molecules on 3-aminopropyltriethoxysilane (APS) SAM with terminal amino group. The dual-layer PFDA–APS film was hydrophobic with the contact angle for water to be about 105° and the overall thickness about 2.5 nm. Atomic force microscopic images revealed that the APS surface was initially characterized with uncontinuous asperities, the surface became relatively smooth and homogeneous after coating with PFDA film by self-assembly. The PFDA–APS film exhibited low

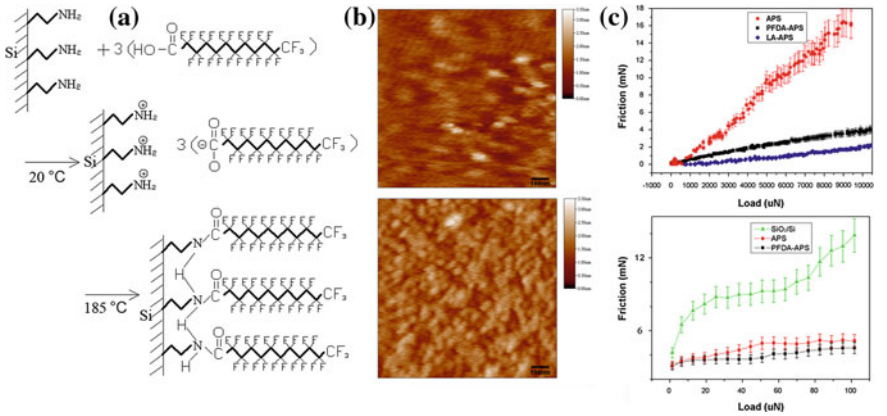

Fig. 3.4 **a** Schematic structure and forming process of PFDA molecules chemically adsorbing onto APS monolayer surface. **b** AFM topographic images of APS monolayer and PFDA–APS dual-layer film on silicon wafer. **c** Microtribological behaviors of the APS monolayer, PFDA–APS dual-layer film and LA–APS dual-layer film surfaces sliding against a steel ball. Reproduced with permission from Ref. [18]. Copyright (2008) Journal of Physical Chemistry C

adhesion and it greatly reduced the friction force at both nano- and microscale. The film exhibited better anti-wear durability than the lauric acid (dodecanoic acid or LA)–APS self-assembled dual-layer film with same chain length and similar structure.

Preparation and Nanotribological Properties of Multi-Component Self-Assembled Dual-Layer Film

Previous results [18–20] indicate that the dual-layer structure can help to improve the film quality and enhance their durability and load bearing capacity. Meanwhile, it is observed that a hydrogenated carboxylic acid dual-layer film exhibits better friction reduction but poorer durability compared to the perfluorinated carboxylic acids dual layer. A lubrication system consisting of dual component self-assembled dual-layer films was designed to minimize friction and a molecular mixture layer to prolong durability. Bai's group [21] reported a novel strategy for a dual-component self-assembled film with control of spatial growth on a large surface area based on a dip-coating nanoparticles method. In selecting among the various SAMs, we particularly focus on the control of both fluorinated and hydrogenated backbone chain molecules because these molecules have strong potential applications in MEMS.

The mechanism of this site-selective growth can be explained as follows. An APS layer was first formed on hydroxylated silicon substrate. Monodisperse Ag

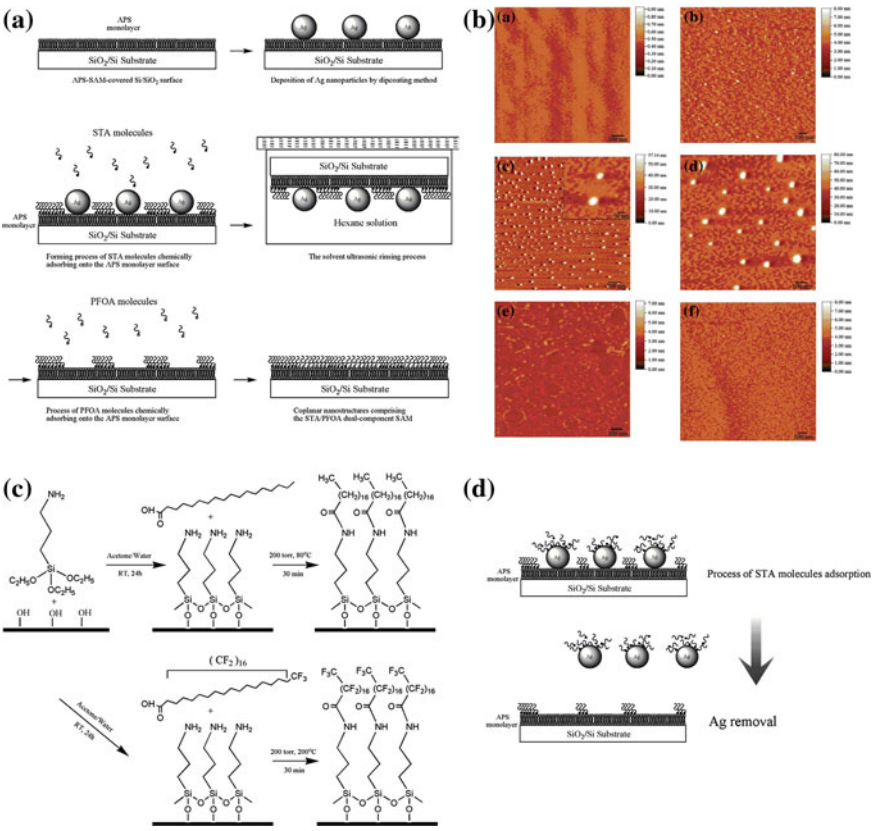

Fig. 3.5 **a** Formation of the coplanar nanostructure STA/PFOA dual-component dual-layer film; **b** AFM images of the film surface in each step; **c** Chemical structure and forming process of STA and PFOA molecules chemically adsorbing onto the APS monolayer surface; **d** Mechanism of STA molecules deposition and Ag nanoparticles removal. Reproduced with permission from Ref. [21]. Copyright (2008) Journal of Physical Chemistry C

nanoparticles capped by long-chain carboxylates played a role in the effective suppression of undesired composite growth on sites. Due to acid amide reaction between stearic acid (STA) and APS molecules, the STA molecules chemisorbed onto the APS-modified surface. The film surface fabricated lunar crater-like pits microstructure and amino-terminated surface exposed in the bottom of the pits after Ag nanoparticles removal. The perfluorooctadecanoic acid (PFOA) molecules absorbed onto the exposed amino terminated surface with acid amide reaction, and the pits of the film were occupied completely by PFOA molecules (Fig. 3.5).

It is important to calculate the spatial distribution of the dual-component film by adhesion statistic measurement, as shown in Fig. 3.6. Adhesive forces of STA and PFOA SAMs were measured as 3.21 and 6.43 nN, respectively. The adhesive

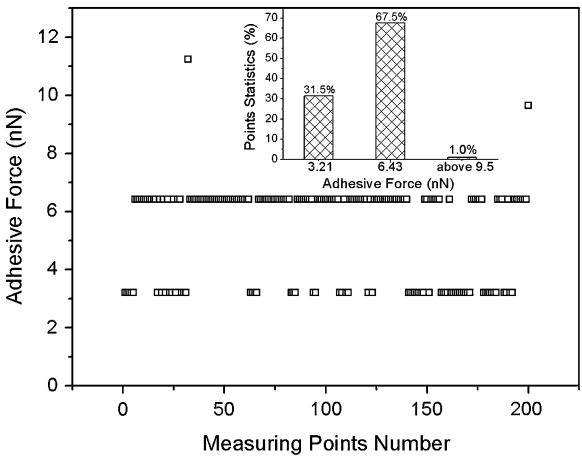

Fig. 3.6 Plot of adhesion force and statistical distribution for the PFOA/STA-APS film (20 °C, 15 % RH). Reproduced with permission from Ref. [21]. Copyright (2008) Journal of Physical Chemistry C

force measurement was typically performed at a rate of 1 Hz along the scan axis and a scan size of 10 × 10 μm during scanning, at least 200 measuring points were carried out for each scan range. From the inset, it can be seen that the adhesive forces of the dual-component layer were calculated statistically as 31.5 and 67.5 %, respectively. The surface coverage of the pits was calculated as a value of about 20 %, which approaches to surface coverage of the pits calculated from the data from the adhesive force measurement. The discrepancy between the surface coverage of pits and the statistical value of PFOA in the adhesion measurement is probably because some STA molecules comprising a SAM exchanged gradually when exposed to the PFOA atmosphere, which results from displacement of SAMs by exchange [22, 23].

Tribolgical Behavior of Multiply-Alkylated Cyclopentane

To utilize SAMs as boundary lubricants, it is necessary to consider the mobile characteristics in addition to the strongly bonded characteristics. The chemically bonded SAMs protect the devices during processing and the early stages of use, while a mobile lubricant is present to replenish the lubricant coating as the SAMs fail. As a result, an ideal boundary lubricant system is pursued.

Multiply-alkylated cyclopentanes (MACs) are composed of one cyclopentane ring with two to five alkyl groups substituted on the ring. They are synthesized by reacting dicyclopentadiene with alcohols of various chain lengths producing a lubricant with a selectable range of physical properties [24]. MAC has excellent viscosity properties, thermal stability and low volatility for use as lubricant and is presently gaining wide acceptance in certain space application [25, 26].

Effect of Wettability on Nanotribology of MACs

Wettability is one of the most important properties of solid surfaces and has attracted much attention since the time of Young in 1805 [27]. It is governed by both chemical composition and topological characteristic of the surface. Controlling wettability is quite important in the study of nanotribological properties.

Wang et al. [28] studied wettability of MACs on silicon substrates that were treated by different cleaning and etching processes. As shown in Fig. 3.7, the wettabilities of MACs on hydroxylated silicon and hydrogenated silicon are better than the wettability on bare silicon without pretreatment, and that outcome is mainly caused by topological structure changes of the surface.

Ma et al. [29] investigated wettability and loading-carrying capacity of MACs on two types of SAMs of decyltrichlorosilane (DTS) and 1H,1H,2H,2H perfluorodecyltrichlorosilane (FDTS). As shown in Fig. 3.8, when MAC was deposited on the DTS-SAM, unlike uniform DTS-SAM, the MAC forms as island-like liquid droplet with a typical diameter of 25 nm and an average height of 3.5 nm was evenly distributed on the DTS-SAM to form dual-layer film with a surface coverage of about 70 %. This research indicate that MAC was deposited on the two SAMs to form dual-layer films with total thickness of 5 nm, the mobile lubricant could markedly decrease friction of DTS-SAM and remarkably promote the load-carrying capacity and durability of both DTS and FDTS SAMs owing to its good self-repairing property.

Distribution and Positioning of Lubricant on a Surface Using the Local Anodic Oxide Method

Local anodic oxidation (LAO) via the atomic force microscope (AFM) is a lithography technique perspective for the fabrication of nanometer-scaled structures and devices. AFM-LAO is based on direct oxidation of the sample by negative voltage applied to the AFM tip with respect to the surface of the sample. The driving force is the faradaic current flows between the tip and sample surface with the aid of the water meniscus. When the faradaic current flows into water bridge, H_2O molecules are decomposed into oxyanions (OH^- and O^-) and protons (H^+). These ions penetrate into the oxide layer because of the high electric field ($E > 107$ V/m), [30] leading to the formation and subsequent growth of SiO_2 on the H-passivated Si surface. The AFM-LAO process can be used not only in fabrication of nanodevices but also in adhesion resistance and friction reduction as in the case of surface texturing. In previous studies [31, 32], AFM-LAO has been demonstrated to be the most promising tool for fabricating nanodots and lines on several types of materials ranging from metals to semiconductors. The LAO process is controlled by several major parameters as follows: pulsed bias voltage, pulsewidth and humidity, as shown in Fig. 3.9.

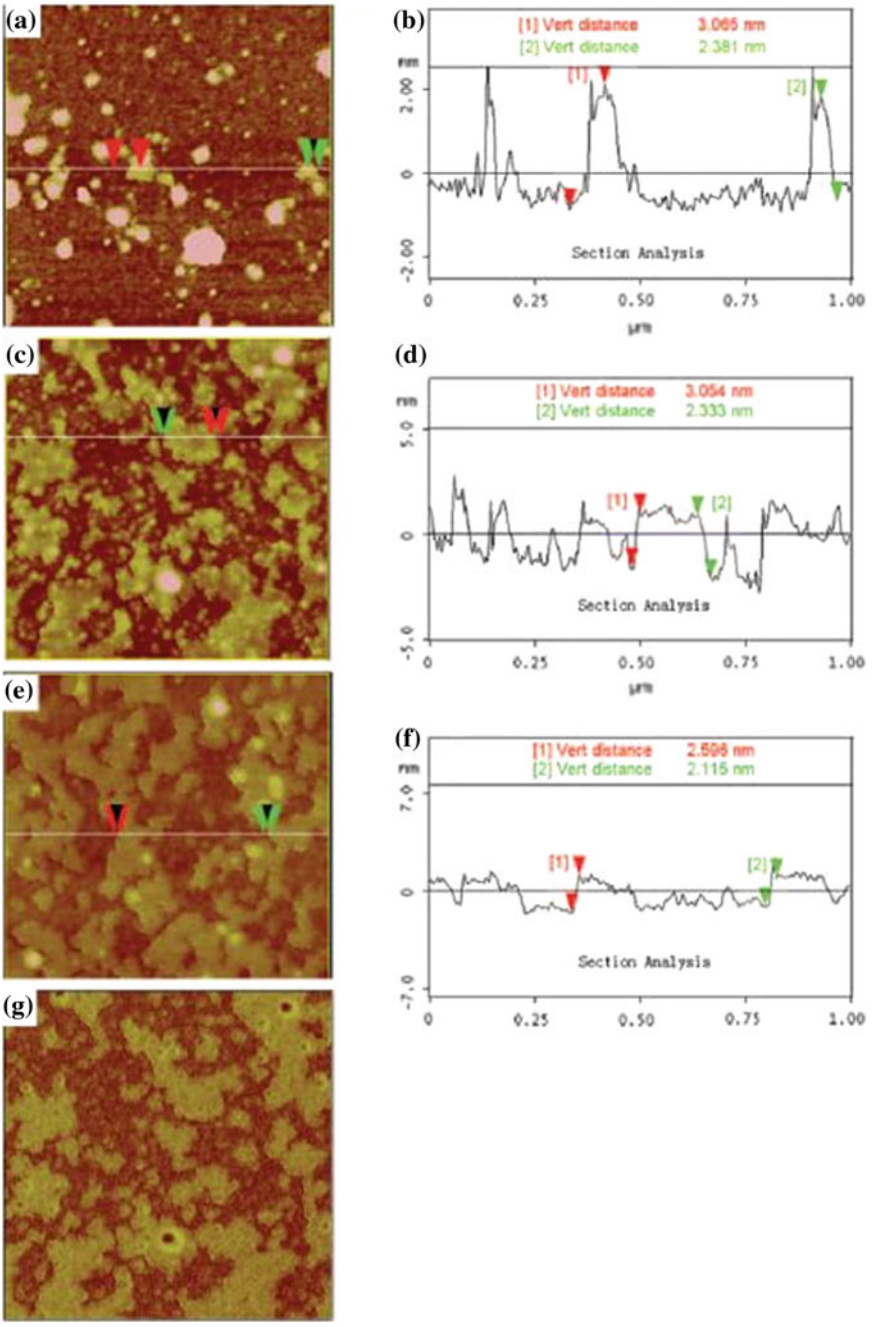

Fig. 3.7 AFM images of MACs films: **a** MACs on bare silicon; **b** line section analysis of (**a**); **c** MACs on hydroxylated silicon; **d** line section analysis of (**c**); **e** MACs on hydrogenated silicon; **f** line section analysis of (**e**); **g** phase map for (**c**). Reproduced with permission from Ref. [28]. Copyright (2010) Tribology Transactions

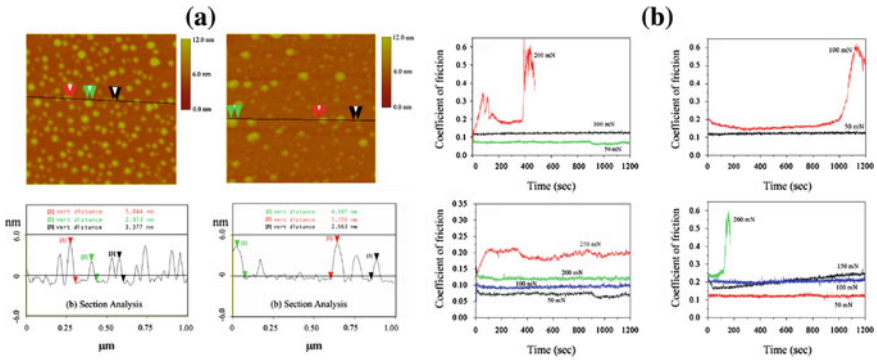

Fig. 3.8 **a** AFM images and section analysis of MAC-DTS dual-layer; **b** friction coefficient and durability of designed SAMs. Reproduced with permission from Ref. [29]. Copyright (2007) Elsevier B. V

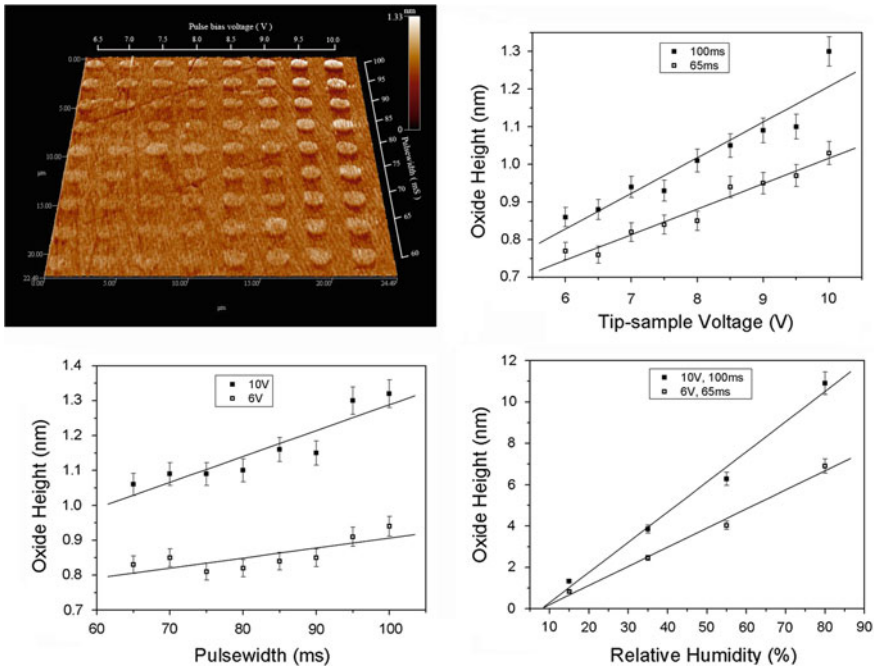

Fig. 3.9 A testing array of Si pillars prepared at different operation parameters, and the oxide height as a function of tip-sample pulse bias voltage, pulsewidth and relative humidity, respectively. Reproduced with permission from Ref. [32]. Copyright (2008) Elsevier B. V

As above mentioned, MAC has excellent viscosity properties, thermal stability, and low volatility for use as a lubricant. Unfortunately, it is difficult to control the size and distribution of lubricants precisely on silicon or DLC. Currently, Bai et al.

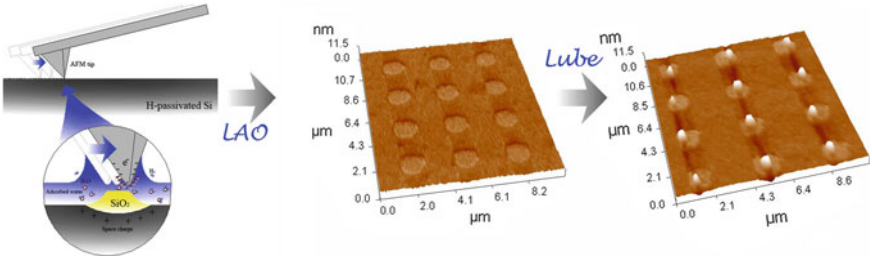

Fig. 3.10 Schematic of distribution and positioning process of MAC on a surface using the local anodic oxide (*LAO*) method. Reproduced with permission from Ref. [33]. Copyright (2009) Langmuir

[33] utilizes an AFM-LAO technique to control the size and distribution of lubricants precisely in an atmospheric environment. The new technique includes two main steps: the production of nanometer-sized nanopatterns using AFM-LAO, followed by the selective adsorption of MAC lubricant onto these patterns using dip-coating method (Figure 3.10).

Ducker [34] first introduced the use of colloidal probe tips by attaching a sphere to the cantilever to measure adhesion. The spherical shape of the tip provides controlled contact pressure, symmetry, and mostly elastic contacts. For adhesion and friction force measurements of the fabricated MAC matrix, the spherical probe tip can fully contact with surface, while sharp tip can only have point contact.

The adhesive force between the colloidal probe and sample surfaces is shown in Fig. 3.11a. A strong adhesive force was observed on the untreated H-passivated silicon surface, on which the adhesive force was about 175 nN. After the patterns were generated, the adhesive force was decreased to 70 nN. This result indicates that the pattern exhibited adhesion resistance. Adhesion is directly related to the bearing ratio, which describes the real area of contact between two solid surfaces. After dip-coating in MAC solution, the adhesive forces of untreated H-passivated

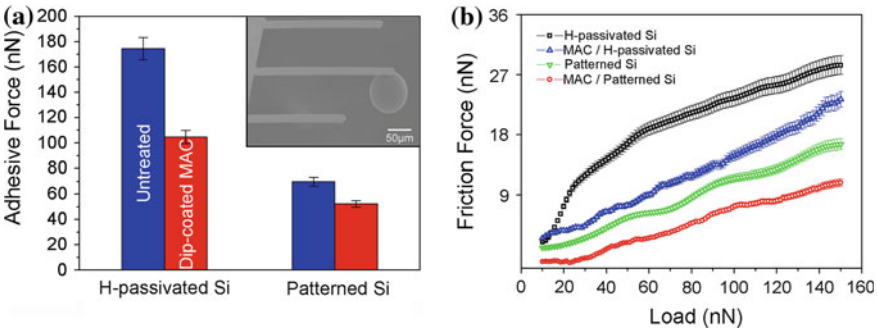

Fig. 3.11 Plots of **a** adhesive forces and **b** friction force between the AFM colloidal probe and the surfaces of samples. The inset shows an SEM image of a typical colloidal probe. Reproduced with permission from Ref. [33]. Copyright (2009) Langmuir

and patterned Si were decreased to 105 and 52 nN, respectively. Such a phenomenon indicates that the MAC layer on the sample surface can obviously lower the interfacial energy and capillarity between the tip and surface. Figure 3.11b presents the plot of friction versus load curves for the bare H-passivated Si and patterned Si and these surfaces treated with MAC. Patterned Si evidently reduced the friction force, and the MAC-cover-patterned Si exhibited the lowest friction force whereas H-passivated Si had a strong friction force. The decrease in friction force is mainly due to a pattern giving rise to a smaller contact area for the same applied load and MAC as the lubricant layer minimizes the shearing strength during sliding.

Tribolgical Behavior of Ionic Liquid Films

Why can ILs be lubricants? ILs have many unique properties, such as negligible volatility at a relatively high temperature, nonflammability, high thermal stability, etc. [35]. These characteristics have attracted great attention and made them available in many potential applications, for example catalysis, electrochemistry, separation science for extraction of heavy metal ions, as solvents for green chemistry, and materials for optoelectronic applications [36–39]. On the other hand, as is well known to tribologists, these characteristics are also just what high performance lubricants demand. Very harsh friction conditions require lubricating oils to have high thermal stability and chemical inertness. The decomposition temperatures of imidazolium ILs are generally above 350 °C, some even as high as 480°C, together with the low temperature fluidity (the glass transition temperature, T_g below 50°C, even 100°C) means that ILs can function in a wide temperature range. In addition, low volatility makes ILs applicable under vacuum, especially for spacecraft application. The above mentioned properties of ILs also make them excellent lubricants. Ye et al. [40, 41] investigated the tribological behavior of two kinds of alkylimidazolium tetrafluoroborate and found them versatile lubricants for the contacts of steel/steel, steel/aluminum, steel/copper, steel/SiO_2, Si_3N_4/SiO_2, steel/Si (100), and steel/sialon ceramics.

Different with large scale mechanical system, MEMS cannot be lubricated with lubrication oils, but can use a thin lubrication film whose thickness is well below a few tens of nanometers. The viscous force comes largely from the viscosity of lubricant films and the meniscus force, rather than the applied loads; this dictates the extent of friction and the mechanisms of lubrication failure. The PFPEs of nanometer thickness are the most widely used lubricants in miniaturized devices, but usually experience metal catalytic degradation and are normally expensive. The potential of ILs in thin film lubrication was exploited by a number of researchers aiming to replace PFPEs [42–46]. The molecular structure, the counter anion, the length of substituted alkyl chains and the functional groups, have key effects on the adhesion and tribological behavior of IL films. The interaction

between lubricant and surface cannot only determine the wetting of lubricant but also determine its durability [47].

Effect of Anion and Substrate Modification

The anions have a more complicated effect on tribological properties in that they cannot only change the viscosity but also surface energy. For ILs with same cations, Zhu et al. [48] demonstrated three kinds of 3-butyl-1-methyl imidazolium ILs with anions of hexafluorophosphate, tetrafluoroborate and adipate as ultra-thin film. Mo et al. [49] introduced a series of propylmethylimidazolium (PMIM) base wear resistant ionic liquid with anions of bromide, carbonate, chloride and sulfite. Adhesion and friction measurements at nanoscale were carried out using a colloidal probe. As shown in Fig. 3.12, based on topography analysis, IL films are found to be prone to attach to the silicon substrate surface, leading to more uniform thin films. Bromide and sulfite anions show favorable lubrication as seen from adhesion and friction, which are less than those of carbonate, chloride and uncoated silicon. The wear test of the IL films was evaluated at loads ranging from 60 to 300 mN and sliding frequency in range 1–20 Hz. IL films showed favorable friction reduction and durability. Imidazolium with anions of chloride and carbonate exhibited a low friction coefficient at a normal load of 200 mN. Imidazolium sulfite exhibits low friction and anti-wear durability even at high-frequency sliding (20 Hz).

Effect of Bonding Percentage and Alkyl Chain Length

The lubricant adsorbed onto silicon after the solvent rinsing process, which is termed as bonding lubricant. The bonding percentages of ionic liquid were measured in terms of the thickness of ionic liquid adsorbed onto silicon surface [%bonding = 100 × (final film thickness/initial film thickness)]. Sinha et al. [50] have also used the similar definition while computing the bonded ratio. To understand the influence of the ratio of bonding to the mobile fraction on the friction in microscale behavior, the mixed IL films were compared with different ratios of bonding to mobile fraction to understand the effect of different bonding percentages. Mo et al. [44] prepared the four kinds of samples (viz. 0, 15, 60 and 85 %) by controlling self-assembled conditions. Fig. 3.13a–e shows the friction coefficients and sliding cycles of 1-alkyl-3-ethylcarboxylic acid imidazolium chloride (AEImi-Cl) ionic liquid with various bonding percentages, as a function of sliding cycles against a steel ball at normal loads ranging between 60 and 500 mN and a sliding velocity of 10 mm/s. Figure 3.13 shows the IL films bonding percentage of 0, 15, 60, and 85 % at a normal load of 60 mN, an average friction coefficient of 0.28, 0.22, 0.18, and 0.16 was recorded, respectively. It was

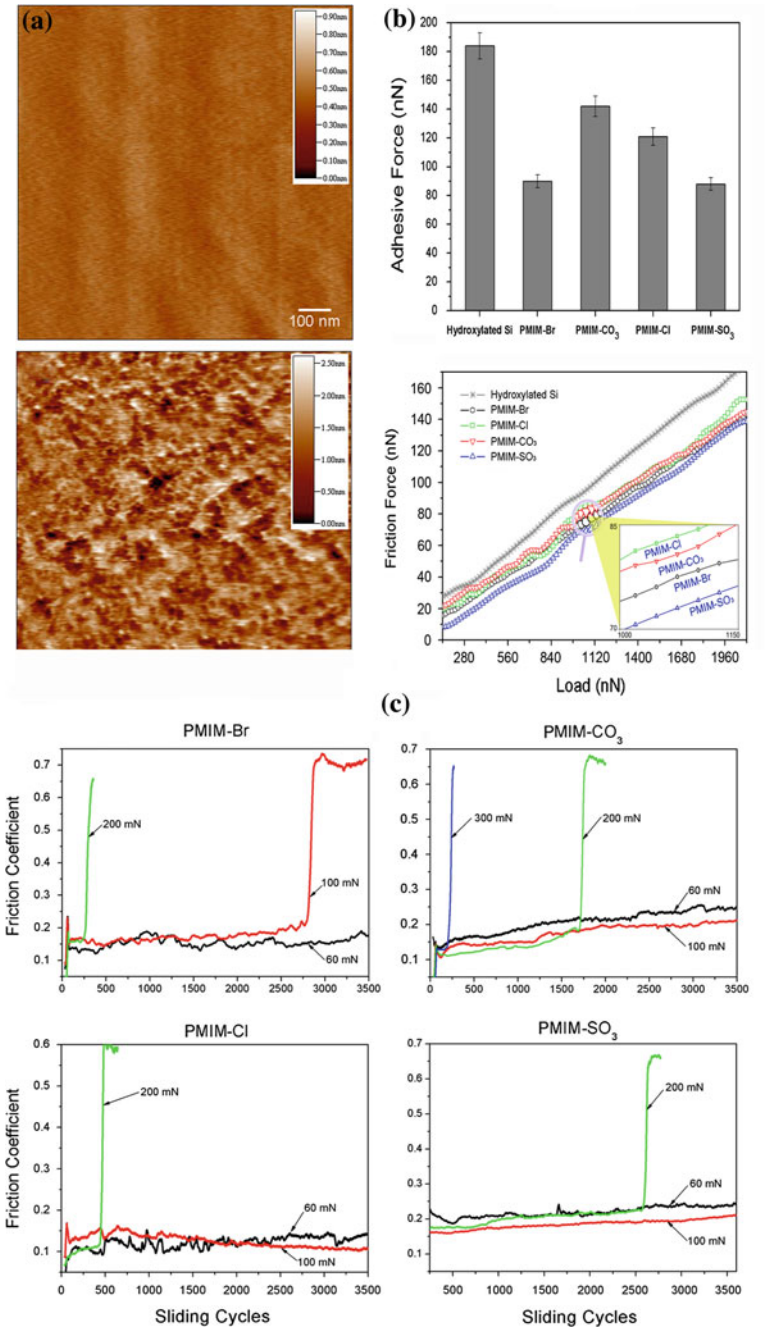

Fig. 3.12 **a** AFM images of hydroxylated Si and IL film surfaces. **b** Adhesive and friction forces between colloidal probe and the surfaces of PMIM-Br, PMIM-CO_3, PMIM-Cl and PMIM-SO_3 IL films. **c** Plots of friction coefficients as function of sliding cycles for PMIM-Br, PMIMOH-CO_3, PMIM-Cl and PMIM-SO_3 film on silicon. Reproduced with permission from Ref. [49]. Copyright (2010) Surface and Interface Analysis

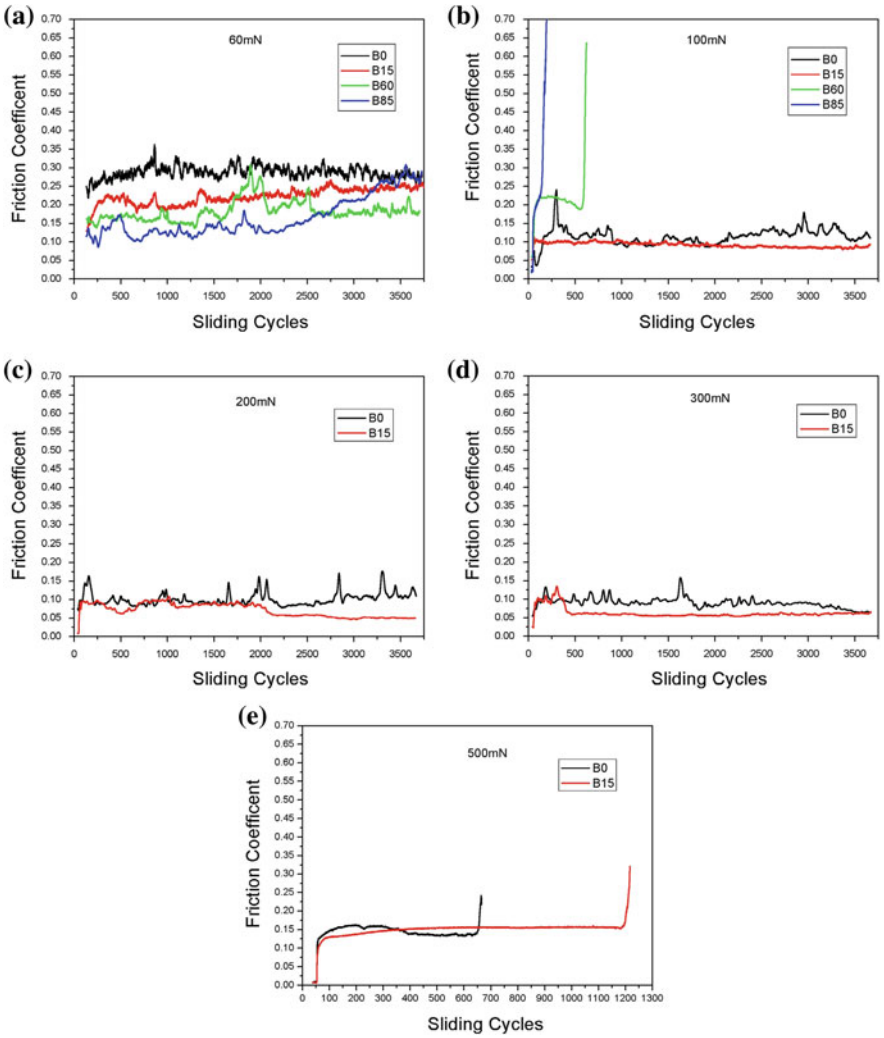

Fig. 3.13 Plots of friction coefficient of AEImi-Cl ionic liquid films with various bonding percentages as function of sliding cycles against steel ball at normal loads of 60, 100, 200, 300, 500 mN with a sliding velocity of 10 mm/s. (The films bonding percentages of 0, 15, 60, and 85 % were denoted as B0, B15, B60, and B85, respectively). Reproduced with permission from Ref. [44]. Copyright (2008) Elsevier B. V

observed that the films with higher bonding percentage exhibited a lower friction coefficient.

The relationship between friction force and external loads for AEImi-Cl ionic liquid with various alkyl chain lengths (viz. C_1, C_4, C_8) is shown in Fig. 3.14. In general, friction is reduced with increase of chain length, and the C_8AEImi-Cl ionic liquid exhibits lowest friction force compared to others. In the formation of

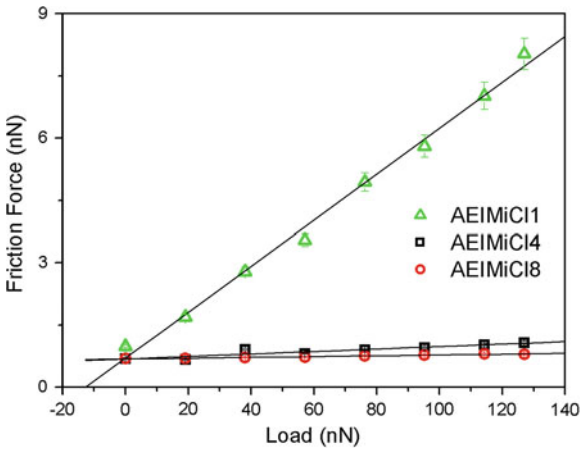

Fig. 3.14 Plots of friction force versus applied loads for AEImi-Cl IL monolayer films with various chain lengths. Reproduced with permission from Ref. [44]. Copyright (2008) Elsevier B. V

the bonding coatings, both the surface energy and inter-chain interactions play important roles and determine quality of the films. Since the AEImi-Cl is the ionic liquid with same terminal group, the nano-friction property is determined by inter-chain interactions.

Effect of Function Group and Annealing Treatment

Zhao et al. [51] successfully prepared four kinds of IL films with different functional cations (1-butyl-3-methylimidazolium hexafluorophosphate, 1-ethanol-3-methylimidazolium hexafluorophosphate, 1-acetic acid -3-methylimidazolium-hexafluorophosphate and 1-phenyl-3-methyl-imidazolium hexafluorophosphate) and characterized their composition and microstructure. The results indicated that IL nanofilms with polar or stiff phenyl cations exhibited relatively higher friction force and better antiwear performance than the ones with apolar alkyl chain structure at micro/nanoscale. The different micro/nanofriction performances of the IL nanofilms were mainly dependent on their different cations which mainly influence their hydrophobic/hydrophilic properties. IL films with more polarized groups generally possessed higher surface energy and a relatively strong interaction during the sliding, and therefore, higher adhesion and more energy loss are expected, which lead to a higher friction force.

Surface morphologies and XPS results [52] indicated that different proportions were formed after post annealing treatment (Fig. 3.15). Annealing treatment of IL film can change the proportions of bonded and mobile molecule in the films. The mobile lubricant fraction present in the partially bonded samples facilitates sliding of the tip on the surfaces; it can rotate with the tip sliding direction easily and

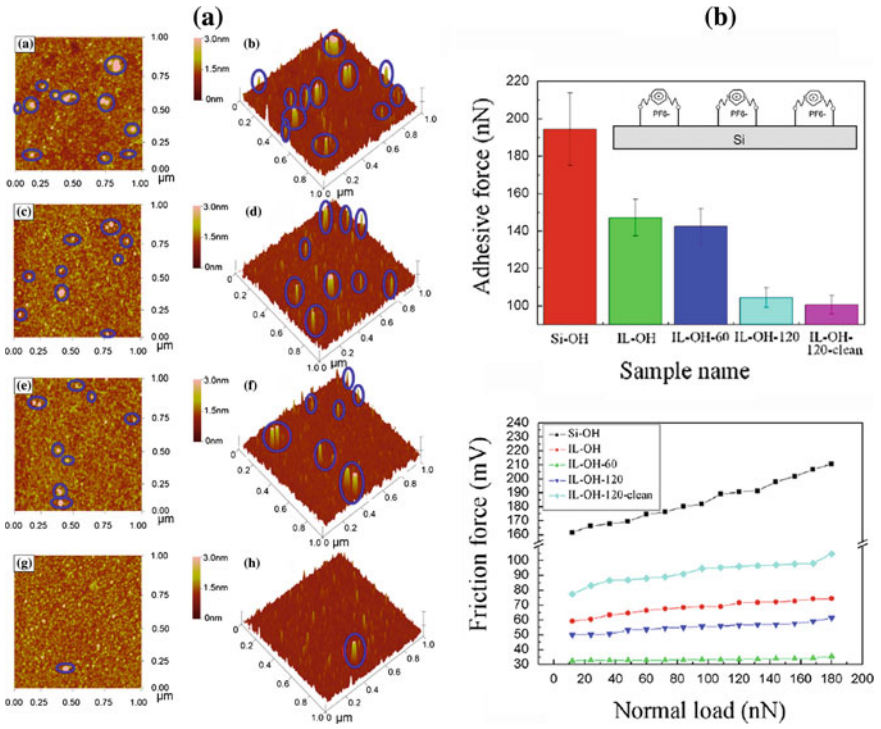

Fig. 3.15 **a** AFM images of IL-OH film at various annealing temperature (from up to down, IL-OH film surfaces are more uniform with reduction in the number of islands); **b** Adhesive and friction force curves of Si, IL-OH films after annealing treatment. Reproduced with permission from Ref. [51]. Copyright (2010) Elsevier B. V

hence the film with higher mobile lubrication fraction exhibits the best nano-tribological performance. Annealing treatment significantly changed friction and adhesion performance at nanoscale.

IL Films with Dual-Layer Structure

Choi et al. [53] prepared mixed lubricants with dual-layer structures on a hydrogenated amorphous carbon surface, which consist of alkylsilane SAMs and mobile PFPE lubricants, and found that the friction and durability properties of the mixed lubricants on the carbon surface were mainly dependent on the alkylsilane monolayers. In order to strengthen bonded fraction and further enhance durability of thin IL film, Pu et al. [54] optimized reaction conditions to achieve partial bonding of ILs to silicon substrate by acid-amide reaction between imidazolium-based ILs carrying carboxylic functional groups and amide-containing SAMs as anchor

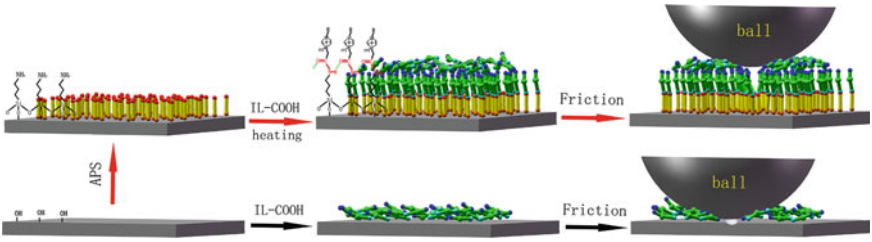

Fig. 3.16 Schematic drawing of the constructing process and frictional mechanism of APS-IL film and IL-COOH film. Reproduced with permission from Ref. [54]. Copyright (2010) Elsevier B. V

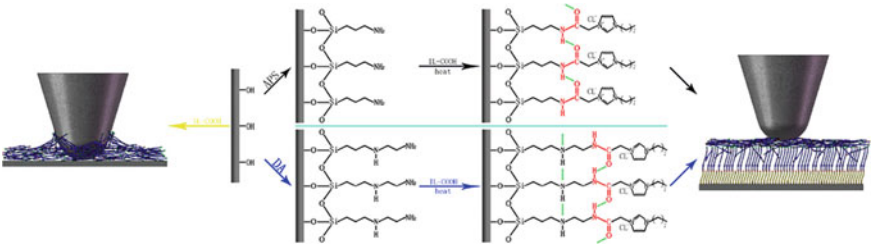

Fig. 3.17 Schematic drawing of the construction process and nanofriction mechanism of APS-IL, DA-IL and IL-COOH films. Reproduced with permission from Ref. [54]. Copyright (2010) Colloids and Surfaces A

layer, and investigated influence of different self-assembled underlayer on the tribological properties of ILs with two-phase structure, aiming to further optimize the nanotribological behaviors of thin IL films and acquire insights into their potential in resolving the tribological problems of MEMS (Figure 3.16).

As shown schematically in Fig. 3.17, a dual-layer film containing both bonded and mobile fractions in IL-COOH layer was constructed on silicon substrates by a two-step process. Two kinds of amino-terminated SAMs which served as anchor layers were formed on hydroxylated silicon surfaces, respectively. Then, the incoming IL-COOH were chemically adsorbed onto amino-terminated SAMs by heat treatment, and formed two-phase structure composed of bonded and mobile IL-COOH molecules.

The formation of chemically bonded phase in IL-COOH layer improves nanotribological properties of the two kinds of dual-layer films as compared with single layer IL-COOH film, which is attributed to synergic effect between mobile phase and steady bonded phase. The protective bonded IL-COOH fraction greatly enhances the stability and antiwear properties of the film, while the mobile IL-COOH fraction serves as lubricant with friction reducing and self-replenishment properties. Generally, the packing density of the underlayer dictates packing density of the overlayer. N-[3-(trimethoxylsilyl)propyl] ethylenediamine (DA)

molecules with longer chains as anchors form more densely packed and orderly SAM as compared with APS, thus more IL-COOH molecules are chemically grafted to DA anchor layer, which produce more densely packed bonded phase and reduce meniscus effect resulted from excessive mobile molecules. These characteristics of DA-IL lead to its lowest friction coefficient among studied dual-layer films. The improved durability of DA-IL film is closely related to high load-carrying capacity of more densely packed and ordered bonded phase. Furthermore, the more interlinked hydrogen bonding further strengthens immobile fraction of dual-layer film.

Enhancement of Nanotribology and Wettability by Surface Textures in Adhesion Resistant

Regular Surface Textures

Nature often uses topographic patterning to control interfacial interactions, such as adhesion and release. Examples range from lotus leaf, gecko to jumping spider. Each example demonstrates that additional to chemistry and material properties, geometric structure is also critical for optimizing interfacial design. Although nature has provided guidance, little is known of how topographic patterns can be intelligently used not only to enhance adhesion but also more importantly to tune adhesion. To tune adhesion with patterns, we must understand how material properties and pattern structure interact. Surface textures and chemical modification are commonly used in magnetic disk drives and MEMS to reduce friction and adhesion in order to reduce the possibility of mechanical failure [55–58]. A number of fabrication methods were used to generate micro/nano-hierarchical structures, including laser/plasma/chemical etching [59], soft photolithography [60], sol–gel processing and solution casting [61], electrical deposition [62], dip-pen printing [63], AFM local anodic oxidation [64], and so on.

Zhao et al. [65] prepared hierarchical structures by replication of textured silicon surfaces using polydimethylsiloxane (PDMS) and self-assembly of alkanethiol [$CH_3(CH_2)_9SH$] to create hydrophobic surface and to improve nanotribological properties of MEMS. As shown in Fig. 3.18, the fabrication technique is a low cost, two-step process, which provides flexibility in fabrication of various hierarchical structures. The textured surface with nano-hierarchical structures can be tailored by adjusting the depth and fractional surface coverage of cylinder hole.

For the adhesive force values there is a decrease when the pillar height and fractional surface coverage increases. Adhesive force also decreased greatly after chemical modification. Compared with the nanopatterned Au surface, the Au surface with micro/nanopillar textures greatly improved the adhesive properties and showed lower adhesive forces. Among the Au surfaces with textures, textured surface with the lowest height of 20 nm were fabricated, and chemical

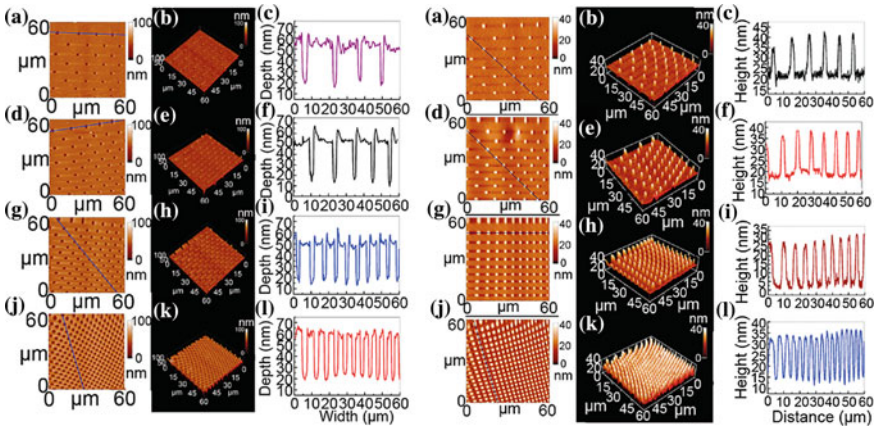

Fig. 3.18 Surface morphologies of template and textured surfaces. Reproduced with permission from Ref. [65]. Copyright (2010) American Chemical Society

modification with ODT-SAMs can lower adhesive force. The results indicate that adhesive force is closely related to the real contact area between the tip and surface, larger area lead to increase adhesive force. With the increase in pillar height and fractional surface coverage, the tip traveling between the pillars results in the decrease of the contact area, responsible for decreased adhesive force. Furthermore, when the solid surfaces were hydrophilic, they would easily form meniscus by the adsorbed water molecules, thus they had larger adhesive force. However, when the surfaces were hydrophobic, they would show lower adhesion (Fig. 3.19).

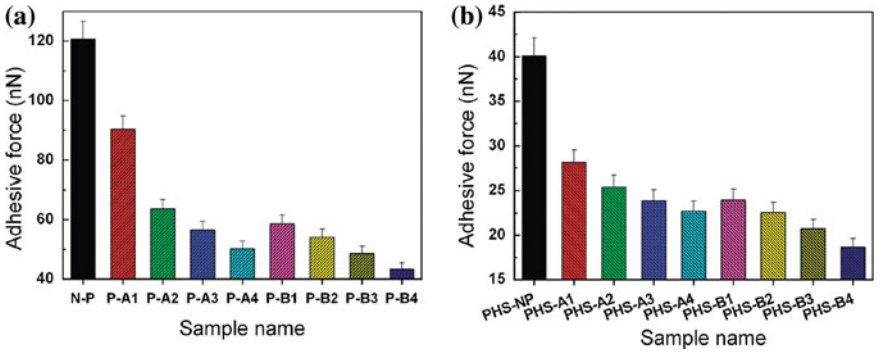

Fig. 3.19 Adhesive forces between AFM tip and Au micro/nano patterned surfaces with different height and surface coverage **a** before and **b** after SAMs chemical modification at room temperature and a relative humidity of 30–40 %. Reproduced with permission from Ref. [65]. Copyright (2010) American Chemical Society

Biomimetic Surface Textures

Functional surfaces with biomimetic micro textures have aroused much interest because of their great advantages in applications such as hydrophobic, anti-adhesion etc. For example, some plant leaves and bodies of animals are known to be hydrophobic in nature because of their intrinsic geometric microstructure. In particular, lotus leaf, on which the water contact angle is larger than 150°, can carry effortlessly the contaminations attached to the leaf when the surface is slightly tilted, which shows self-cleaning function and low hysteresis.

Wang et al. [66] reported three surface micro textures of rice leaf, lotus leaf and snake skin, which were duplicated on surface by combining duplication and electroplating methods. Firstly, a cellulose film is used to replicate the surface micro textures of the biological sample to obtain a negative impression of the biomimetic textures [67, 68]. A metallic layer is electrodeposited on the top of the cellulose film. Then the positive replicas of the original living creature were obtained after removing the cellulose film. Using this method, they successfully duplicated the surface microtextures of the rice leaf, lotus leaf and the snake skin on surface and evaluated wettability of the surfaces (Fig. 3.20). Zhao et al. [69] also used a simple, efficient, and highly reproducible method for producing large-area positive and negative lotus and rice leaf topography on Au surfaces based on PDMS to enhance hydrophobicity.

Mo et al. [70] successfully fabricated biomimetic textures onto silicon surface by local anodic lithography. Furthermore, the dimensions of biomimetic textures can be precisely controlled by controlling pulsed bias voltage, pulse width and RH, as shown in Fig. 3.21.

In this approach, the surfaces of dung beetle and rice leaf were replicated on H-passivated Si surface. The experimental results show that the lowest value of the

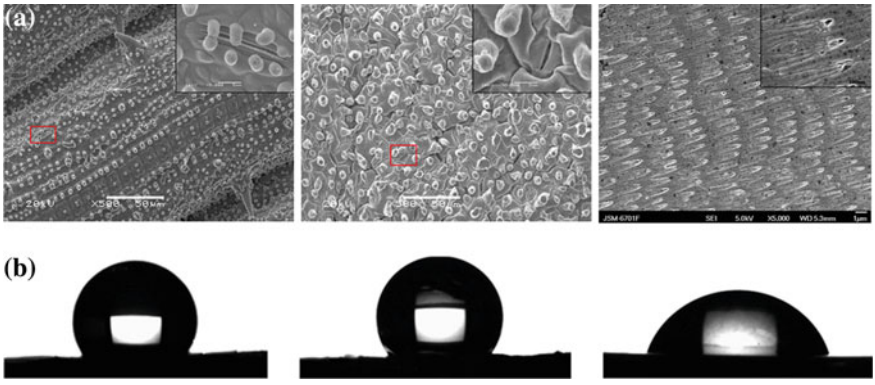

Fig. 3.20 **a** SEM images of surface replica of rice leaf, and on surface. The insets are the high magnification images. **b** Water droplet on surface replica with different textures (157° for rice leaf, 161° for lotus leaf and 65° for snake skin). Reproduced with permission from Ref. [66]. Copyright (2010) Elsevier B. V

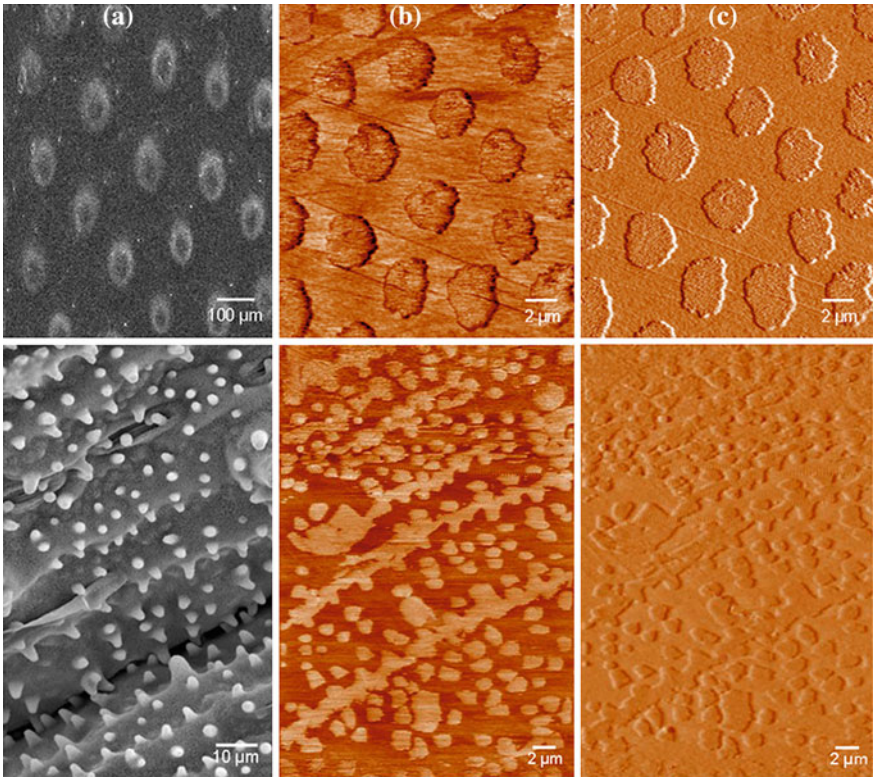

Fig. 3.21 The SEM image **a** of the surface replica of dung beetle and rice **b** Topographic scan of the replica **c** Corresponding frictional force image of (**b**). Reproduced with permission from Ref. [70]. Copyright (2010) Elsevier B. V

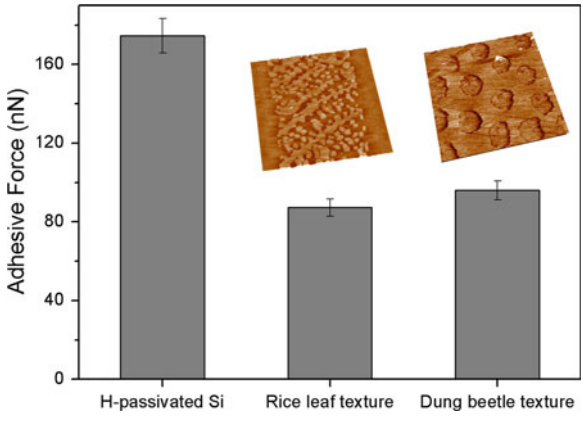

Fig. 3.22 Adhesive forces between AFM colloidal probe and surfaces of bare H-passivated Si, rice leaf texture and dung beetle texture. Reproduced with permission from Ref. [70]. Copyright (2010) Elsevier B. V

height of the biomimetic nanotexture was about 1 nm. The H-passivated Si treated with biomimetic nanotextures exhibit better adhesive resistance than untreated Si at nanoscale (Fig. 3.22). It is expected that this approach could be extended to duplicate other biological and artificial template surfaces on silicon surface. These surfaces with special nanotextures are of great importance for MEMS practical applications such as microhydromechanics, wettability, and biochips.

Summary and Outlook

Part of the excitement in thin lubricant film is due to the great intellectual simplification associated with the routine way. In this chapter, we have tried to introduce those ideas and concepts. Perfluorinated SAMs have shown remarkably better lubrication and anti-adhesion properties. A comparative research is presented on the surface and nanotribological properties of FC and HC SAMs on aluminum-coated silicon substrate formed by chemical vapor deposition. Furthermore, the influence of environmental conditions, such as RH and temperature, on tribological performance of these SAMs, was investigated. The FC SAMs show obvious environmental independence. In addition, dual-layer film exhibits better anti-wear durability than single monolayer in nanoscale.

MACs and ILs also are potential lubricants for MEMS and space application due to their extreme low volatility. In recent progress we have described important fields of boundary lubrication and the friction of single asperity contact. In ambient conditions, as well as in many tribological applications, surfaces are often covered by a thin film which modifies their tribological properties. Liquid menisci may form, increasing the adhesive force between the contact surfaces. The physical and chemical interactions between the surfaces are affected by the presence of water which can act as a lubricant. The tribological properties of the surface can also be changed directly by covering the surface with a monolayer of organic materials (SAMs with different function group or ILs with different ions). Meanwhile, surface texture is a prospective physical approach to enhance wettability and nanotribology in adhesion resistant conditions.

Summarizing, nanotribology of molecular thin films is a young and emerging field that is maturing fast, as the experiments described show. Due to never ending trend to miniaturization, understanding friction at nanoscale will become of increasing importance, since as the length scale is reduced, friction force become stronger relative to surface force, and thin films may be the only way to lubricate. If a bridge between nano- and macroscopic tribology is found, thin film with a molecular thickness might improve more efficiency and durability of MEMS.

Acknowledgments This work was funded by the National Natural Science Foundation of China (NSFC) under Grant No. 11172300 and 51105352. Prof. Mingwu Bai and Prof. Qunji Xue are greatly acknowledged for their constant support and encouragements to carry out this research work.

The authors want to express their sincere gratitude to Dr. Chongjun Pang, Dr. Jianqi Ma, Dr. Min Zhu, Dr. Wenjie Zhao, Dr. Ying Wang, Dr. Jibin Pu for their great efforts and valuable discussions.

References

1. Mo, Y., Bai, M.: Surf. Interface Anal. **41**, 602 (2009)
2. Hutt, D.A., Leggett, G.J.: Langmuir **13**, 2740 (1997)
3. Wallace, R., Chen, P., Henck, S., Webb, D.: J. Vac. Sci. Technol. A **13**, 1345 (1995)
4. Chance, J.J., Purdy, W.C.: Langmuir **13**, 4487 (1997)
5. Miura, Y.F., Takenaga, M., Koini, T., Graupe, M., Garg, N., Graham, R.L., Lee, T.R.: Langmiur **14**, 5821 (1998)
6. Xiao, X.D., Hu, J., Charych, D.H., Salmeron, M.: Langmuir **12**, 235 (1996)
7. Ren, S., Yang, S., Zhao, Y., Zhou, J., Xu, T., Liu, W.: Tribol. Lett. **13**, 233 (2002)
8. Ruehe, J., Novotny, V.J., Kanazawa, K.K., Clarke, T., Street, G.B.: Langmuir **9**, 2383 (1993)
9. Patton, S.T., William, D.C., Eapen, K.C., Zabinski, J.S.: Tribol. Lett. **9**, 199–209 (2000)
10. Rye, R.R., Nelson, G.C., Dugger, M.T.: Langmuir **13**, 2965–2972 (1997)
11. Hsu, S.M.: Tribol. Int. **37**, 537–545 (2004)
12. Tam-Chang, S.-W., Biebuyck, H.A., Whitesides, G.M., Jeon, N., Nuzzo, R.G.: Langmuir **11**, 4371 (1995)
13. Clegg, R.S., Hutchison, J.E.: J. Am. Chem. Soc. **121**, 5319 (1999)
14. Clegg, R.S., Reed, S.M., Smith, R.K., Barron, B.L., Rear, J.A., Hutchison, J.E.: Langmuir **15**, 8876 (1999)
15. Chambers, R.C., Inman, C.E., Hutchison, J.E.: Langmuir **21**, 4615 (2005)
16. Song, S., Ren, S., Wang, J., Yang, S., Zhang, J.: Langmuir **22**, 6010 (2006)
17. Song, S., Zhou, J., Qu, M., Yang, S., Zhang, J.: Langmuir **24**, 105 (2008)
18. Mo, Y., Zhu, M., Bai, M.: Colloids Surf. A: Physicochem. Eng. Aspects **322**, 170 (2008)
19. Ren, S.L., Yang, S.R., Zhao, Y.P.: Langmuir **19**, 2763 (2003)
20. Ma, J., Pang, C., Mo, Y., Bai, M.: Wear **2007**, 263 (1000)
21. Mo, Y., Bai, M.: J. Phys. Chem. C **112**, 11257 (2008)
22. Fleming, M.S., Walt, D.R.: Langmuir **17**, 4836 (2001)
23. Love, J.C., Estroff, L.A., Kriebel, J.K., Nuzzo, R.G., Whitesides, G.M.: Chem. Rev. **105**, 1103 (2005)
24. Venier, C.G., Casserly, E.W.: US 4,929,782, 1990
25. Venier, C.G., Casserly, E.W.: Lubr. Eng. **47**, 586 (1991)
26. Dube, M.J., Bollea, D., Jones Jr, W.R., Marrcheti, M., Jansen, M.J.: Tribol. Lett. **15**, 3–8 (2003)
27. Young, T.: Philos. Trans. R. Soc. Lond. **95**, 65 (1805)
28. Wang, Y., Mo, Y., Zhu, M., Bai, M.: Tribol. Trans. **53**, 219 (2010)
29. Ma, J., Liu, J., Mo, Y., Bai, M.: Colloids Surf A: Physicochem. Eng. Aspects **301**, 481 (2007)
30. Jian, S.R., Fang, T.H., Chuu, D.S.: J. Phys. D Appl. Phys. **38**, 2432 (2005)
31. Garcia, R., Martinez, R., Martinezz, J.: Chem Soc Rev **35**, 29 (2006)
32. Mo, Y.F., Wang, Y., Bai, M.W.: Phys. E **41**, 146 (2008)
33. Mo, Y., Wang, Y., Pu, J., Bai, M.: Langmuir **25**, 40 (2009)
34. Ducker, W.A., Senden, T.J., Pashley, R.M.: Nature **353**, 239 (1991)
35. Hagiwara, R., Ito, Y., Fluorine, J.: Chem. **105**, 221 (2000)
36. Welton, T.: Chem. Rev. **99**, 2071 (1999)
37. Wasserscheid, P., Keim, W.: Angew. Chem. Int. Ed. **39**, 3772 (2000)
38. Earle, M.J., Seddon, K.R.: Pure Appl. Chem. **72**, 1391 (2000)
39. Nakashima, T., Kawai, T.: Chem. Commun. **12**, 1643 (2005)
40. Ye, C.F., Liu, W.M., Chen, Y.X., Yu, L.G.: Chem. Commun. **21**, 2244 (2001)
41. Liu, W.M., Ye, C.F., Gong, Q.Y., Wang, H.Z., Wang, P.: Tribol. Lett. **13**, 81 (2002)

42. Palacio, M., Bhushan, B.: Adv. Mater. **20**, 1194 (2008)
43. Yu, G., Zhou, F., Liu, W.M., Liang, Y.M., Yan, S.: Wear **2006**, 260 (1076)
44. Mo, Y., Bo, Y., Zhao, W., Bai, M.: Appl. Surf. Sci. **255**, 2276 (2008)
45. Yu, B., Zhou, F., Mu, Z., Liang, Y.M., Liu, W.M.: Tribol. Inter. **39**, 879 (2006)
46. Bhushan, B., Palacio, M., Kinzig, B.: J. Colloid Interface Sci. **317**, 275 (2008)
47. Zhou, F., Liang, Y., Liu, W.: Chem. Soc. Rev. **38**, 2590–2599 (2009)
48. Zhu, M., Yan, J., Mo, Y., Bai, M.: Tribol. Lett. **29**, 177 (2008)
49. Mo, Y., Zhao, W., Zhu, M., Bai, M.: Tribol. Lett. **32**, 143 (2008)
50. Sinha, S.K., Kawaguchi, M., Kato, T., Kenedy, F.E.: Tribol. Int. **36**, 217 (2003)
51. Zhao, W., Wang, Y., Wang, L., Bai, M., Xue, Q.: Colloids Surf. A: Physicochem. Eng. Aspects **361**, 118 (2010)
52. Xiao, X.D., Hu, J., Charych, D.H., Salmeron, M.: Langmuir **12**, 235 (1996)
53. Choi, J., Kawaguchi, M., Kato, T.: Tribol. Lett. **15**, 353 (2003)
54. Pu, J., Huang, D., Wang, L., Xue, Q.: Colloids Surf. A: Physicochem. Eng. Aspects **372**, 155 (2010)
55. Marchetto, D., Rota, A., Calabri, L., Gazzadi, G.C., Menozzi, C., Valeri, S.: Wear **265**, 577 (2008)
56. Pettersson, U., Staffan, J.: Tribol. Int. **36**, 857 (2003)
57. Wakuda, M., Yamauchi, Y., Kanzaki, S., Yasuda, Y.: Wear **254**, 356 (2003)
58. Suh, A.Y., Lee, S.C., Polycarpou, A.A.: Tribol. Lett. **17**, 739 (2004)
59. Laws, G.M., Handugan, A., Eschrich, T., Boland, P., Sinclair, C., Myhajlenko, S., Poweleit, C.D.: J. Vac. Sci. Technol. B **25**, 2059 (2007)
60. Xu, Q.B., Tonks, I., Fuerstman, M.J., Love, J.C., Whitesides, G.M.: Nano. Lett. **4**, 2509 (2004)
61. Bhushan, B., Kocha, K., Jung, Y.C.: Soft Matter **4**, 1799 (2008)
62. Shirtcliffe, N.J., McHale, G., Newton, M.I., Chabrol, G., Perry, C.C.: Adv. Mater. **2004**, 16 (1929)
63. Zheng, Z., Daniel, W.L., Giam, L.R., Huo, F., Senesi, A.J., Zheng, G., Mirkin, C.A.: Angew. Chem. Inter. Ed, **48**(41), 7626
64. Garcia, R., Martinez, R.V., Martinez, J.: Chem. Soc. Rev. **35**, 29 (2006)
65. Zhao, W., Wang, L., Xue, Q.: ACS Appl. Mater Interfaces **2**, 788 (2010)
66. Wang, Y., Mo, Y., Zhu, M., Bai, M.: Surf. Coat. Technol. **203**, 137 (2008)
67. Zhao, X.M., Xia, Y., Whitesides, G.M.: J. Mater. Chem. **1997**, 7 (1069)
68. Sun, M.H., Luo, C.X., Xu, L.P., Ji, H., Ouyang, Q., Yu, D.P., Chen, Y.: Langmuir **21**, 8978 (2005)
69. Zhao, W., Wang, L., Xue, Q.: J. Phys. Chem. C **114**, 11509 (2010)
70. Mo, Y., Bai, M.: J. Colloid Interface Sci. **333**, 304 (2009)